International Journal of Bridge Engineering (IJBE), Vol. 6, No. 1, (2018), pp. 91-105

SUSPENDED ARCH BRIDGES UNDER MOVING LOADS

The 2D mathematical model

Theodore G. Konstantakopoulos[1] and George T. Michaltsos[2]

[1]Civil Engineer PhD N.T.U.A., Greece
[2]National Technical University of Athens, Dept. of Civil Engineering, Greece
e-mail: theokons@teemail.gr, michalts@central.ntua.gr

ABSTRACT: The present work studies the behavior of a suspended arch bridge under the action of concentrated or distributed moving loads, proposing a mathematical model for the problem. The studied suspended arch bridge has a dense arrangement of cables, while the described method can easily be extended in the case of a sparse arrangement of cables.

A 2D model is considered for the study of the bridge, while the theoretical formulation, is based on a continuum approach that has been used in the literature to analyze such bridges. Finally the obtained equations are solved using the Laplace Transform.

KEYWORDS: Suspended Arch bridges; Dynamic of bridges; Moving loads.

1 INTRODUCTION

Arches provide a structural system that can efficiently support large loads while lending themselves to excellent aesthetics. Historically, arches have been widely used in bridge systems; however, in modern applications they are usually reserved for signature bridges, where aesthetics play an important role in the design. Because arches primarily resist loads through compression, steel and also concrete are ideal structural materials for their application.

In the last decades, the design practice for various types of steel structures, have been changed to limit state design rules to obtain more rational designs.

As for the steel arch structures, the classical critical instability is often regarded as the chief design criterion [1]. However, this is by no means the ultimate load, which the arches with practical proportioning can carry.

The papers studying the actual carrying capacity of arches with practical proportioning under practical loadings (i.e. circulation loads, earthquake's loads, support's motion etc), are considerably less than the ones studying the classical bifurcation buckling.

Among the studies relating to stability one should mention the Johnston's

study [1] and also those of Bergermeister et al [2], Pircher et al [3], Wang et al [4], Zhu and Sun [5], Bruno et al [6], Mannini et al [7] etc.
Among the studies relating to the creep phenomenon there is a lot of papers [8 to 15] relating, mainly, to the creep of concrete-filled steel arch tubes.

The actual carrying capacity of arches with practical proportioning under practical earthquake loadings is considerably less than those relating to the classical bifurcation buckling [16 to 20].

Finally, there is a lack of papers relating to the supports' settlement and moving loads.

As for the supports' settlement, Drosopoulos et al [22] studied the behavior of stone arch bridge subjected to the abutment movement while Liu et al [22] studied the effect of a springing displacement.

As for the moving loads, there are papers related to masonry arch bridges [23] or hanger arch bridges [24-25] while the papers relating to the classical form of an arch bridge use numerical methods [26] or F.E. ones [27]. Few publications study the influence of moving trains as for example the paper of Calcada et al [28], Cher t al [29] or Wallin et al [30].

An arch bridge consists of three elements: the deck, the arch, and the cables (hangers) that connect deck and arch.

Although it is usual the dense arranged cables to be considered no deformable, in this study we consider them deformable in order to study their real behavior. In addition an initial lifting (negative deformation) of the deck has been considered, i.e. an initial tension of the cables in order to avoid the possible appearing compressive stresses.
Finally the form of the parabolic arch is given by the equation:

$$z(x) = \frac{4 \cdot f_o}{L^2} \cdot x^2 - \frac{4 \cdot f_o}{L} \cdot x \tag{1}$$

The present work studies the behavior of a suspended arch bridge under the action of concentrated or distributed moving loads, proposing a mathematical model for the problem. The studied suspended arch bridge has a dense arrangement of cables, while the described method can easily be extended in the case of a sparse arrangement of cables.

A 2D model is considered for the study of the bridge while the theoretical formulation, is based on a continuum approach, that has been used in the literature to analyze such bridges. Finally the obtained equations are solved using the Laplace Transform.

A variety of numerical examples allow one to draw important conclusions for structural design purposes.

2 INTRODUCTORY CONSEPTS

2.1 The arch

Let us consider the arch beam of figure 1, which the form is given by the

following equation:

$$z = z(x) \tag{2a}$$

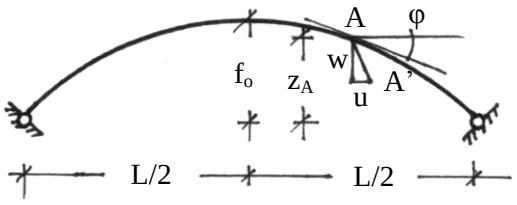

Figure 1. The arch

From the initial and the deformed state of an infinitesimal part ds of the arch we find:

$$\left.\begin{aligned} dx + du &= (1+\varepsilon)\cdot ds\cdot\cos(\varphi+\psi) \cong dx + \varepsilon\cdot dx - \psi\cdot dz \\ dz + dw &= (1+\varepsilon)\cdot ds\cdot\sin(\varphi+\psi) \cong dz + \varepsilon\cdot dz + \psi\cdot dx \end{aligned}\right\}$$

Or finally:

$$\left.\begin{aligned} du &= \varepsilon\cdot dx - \psi\cdot dz \\ dw &= \psi\cdot dx + \varepsilon\cdot dz \end{aligned}\right\} \tag{2b}$$

where infinitesimal of higher order $\boldsymbol{(\varepsilon\cdot dz\cdot\psi,\ \ \varepsilon\cdot dz\cdot dx)}$ are neglected.
For a non-extensible beam (ε=0) we have:

$$\left.\begin{aligned} \frac{d\psi}{ds} &= \frac{d^2w}{dx^2}\cdot\frac{dx}{ds} \\ \frac{du}{dx} &= \varepsilon\cdot\left[1+\left(\frac{dz}{dx}\right)^2\right] - \frac{dw}{dx}\cdot\frac{dz}{dx} \end{aligned}\right\} \tag{2c}$$

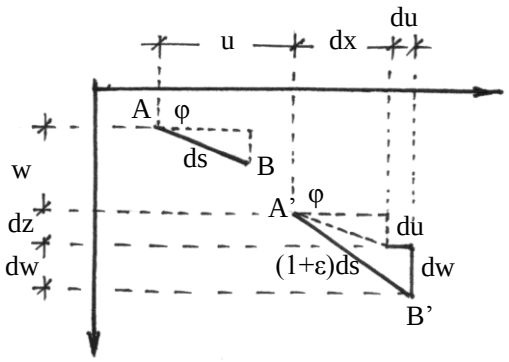

Figure 2. Deformation of an infinitesimal part ds

From the second of the above (2c) we obtain:

$$\int_0^L du = u(L) - u(0) = \int_0^L \varepsilon \cdot (1 + z'^2) dx - \int_0^L z' \cdot w' dx = 0$$

which after integration gives (because $w(0) = w(L) = u(0) = 0$):

$$\int_0^L \varepsilon \cdot (1 + z'^2) dx + \int_0^L z'' \cdot w dx = 0 \tag{2d}$$

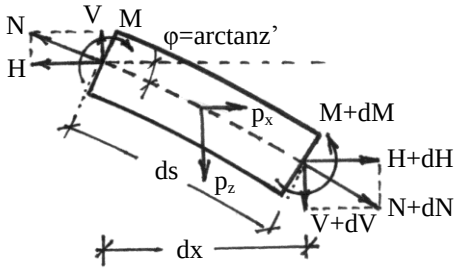

Figure 3. Equilibrium of an infinitesimal part ds

From figure 3 we get $dH = -p_x dx$ and because it is usually $p_x = 0$, we obtain:
On the other hand we know that:

$$\left.\begin{aligned} \varepsilon = \frac{N}{E \cdot A(x)}, \quad 1 + z'^2 = \frac{1}{\cos^2 \varphi}, \quad N = \frac{H}{\cos \varphi} \end{aligned}\right\} \tag{2e}$$

Therefore, equation (2d) becomes:

$$\int_0^L \frac{N}{E \cdot A(x) \cdot \cos^2 \varphi} dx = \int_0^L \frac{H}{E \cdot A(x) \cdot \cos^3 \varphi} dx = -\int_0^L z'' \cdot w dx \tag{2f}$$

$$H = constant \tag{3a}$$

And thus:

$$\left.\begin{aligned} H &= -\frac{1}{K} \cdot \int_0^L z'' \cdot w dx \\ \text{where: } K &= \int_0^L \frac{dx}{EA(x) \cos^3 \varphi} \end{aligned}\right\} \tag{3b}$$

From the equilibrium of figure 3 we conclude to the following equations:

$$\left.\begin{aligned} z''H = -p_z, \quad \frac{dV}{dx} = -p_z, \quad \frac{d^2M}{dx^2} = H \cdot (z - w)'' + p_z \end{aligned}\right\} \tag{3c}$$

From the first of (2c) we get: $\frac{d\psi}{ds}=\frac{d^2w}{dx^2}\cdot\frac{dx}{ds}=-\frac{M}{E\,I_a}$ or $\frac{d^2w}{dx^2}=-\frac{M}{E\,I_a\cos\varphi}$

while because of (3c) and taking into account the inertia forces we obtain:

$$\frac{d^2}{dx^2}\left(E\,I_a\cos\varphi\frac{d^2w_a}{dx^2}\right)+H\cdot w_a''+m_a\ddot{w}_a=p_z-\frac{z''}{K}\cdot\int_0^L z''\cdot w_a dx \qquad (3d)$$

From equation (1) we find $z''=8f_o/L^2$ while we put, as usual, $I_a\cos\varphi=I_c$ where I_c is the moment of inertia at the top point of the arch. Therefore equation (3d) becomes:

$$E\,I_c w_a''''-\frac{mgL^2}{8f_o}w_a''+m_a\ddot{w}_a=p_z-\frac{64f_o^2}{KL^4}\int_0^L w_a dx \qquad (3e)$$

Putting $p_z=0$, we get the equation of the free motion from which we will try to determine the eigenfrequencies and the shape functions of the arch:

$$E\,I_c w_a''''-\frac{mgL^2}{8f_o}w''+m_a\ddot{w}_a=-\frac{64f_o^2}{KL^4}\int_0^L w_a dx \qquad (4a)$$

We are searching for a solution of the form:

$$w_a(x,t)=W(x)\cdot e^{i\omega t} \qquad (4b)$$

Therefore equation (4a) becomes:

$$\left.\begin{aligned} &W''''-A\cdot W''-k^4W=-B\int_0^L W\,dx \\ &\text{where:}\quad A=\frac{mgL^2}{8f_oEI_c},\quad B=\frac{64\,f_o^2}{KL^4EI_c},\quad k^4=\frac{m_a\omega^2}{EI_c} \end{aligned}\right\} \qquad (4c)$$

Given that the integral of the right site member is independent of x, the general solution of (4c) will be:

$$\left.\begin{aligned} &W(x)=c_1\sin\lambda_1x+c_2\cos\lambda_1x+c_3\mathrm{Sinh}\lambda_2x+c_4\mathrm{Cosh}\lambda_2x+\frac{B}{k^4}\int_0^L W dx \\ &\text{with:}\quad \lambda_1=\sqrt{-\frac{A}{2}+\sqrt{\frac{A^2}{4}+k^4}},\quad \lambda_2=\sqrt{\frac{A}{2}+\sqrt{\frac{A^2}{4}+k^4}} \end{aligned}\right\} \qquad (4d)$$

Integrating (4d) we find:

$$\int_0^L W dx = \frac{k^4}{k^4 - BL} \cdot \left[-\frac{c_1}{\lambda_1}(\cos\lambda_1 L - 1) + \frac{c_2}{\lambda_1}\sin\lambda_1 L + \frac{c_3}{\lambda_2}(\mathrm{Cosh}\lambda_2 L - 1) + \frac{c_4}{\lambda_2}\mathrm{Sinh}\lambda_2 L \right]$$

Therefore the final solution of equation (4c) becomes:

$$\left.\begin{aligned} W(x) = c_1\left[\sin\lambda_1 x - \frac{B}{\lambda_1(k^4 - BL)}(\cos\lambda_1 L - 1)\right] + c_2\left[\cos\lambda_1 x + \frac{B}{\lambda_1(k^4 - BL)}\sin\lambda_1 L\right] \\ + c_3\left[\mathrm{Sinh}\lambda_2 x + \frac{B}{\lambda_2(k^4 - BL)}(\mathrm{Cosh}\lambda_2 L - 1)\right] + c_4\left[\mathrm{Cosh}\lambda_2 x + \frac{B}{\lambda_2(k^4 - BL)}\mathrm{Sinh}\lambda_2 L\right] \end{aligned}\right\} \quad (4e)$$

With boundary conditions $W(0) = W(L) = W''(0) = W''(L) = 0$, we obtain the following equation for eigenfrequencies:

$$\begin{vmatrix} -\frac{B}{\lambda_1(k^4 - BL)}(\cos\lambda_1 L - 1) & \left(1 + \frac{B}{\lambda_1(k^4 - BL)}\sin\lambda_1 L\right) & \frac{B}{\lambda_2(k^4 - BL)}(\mathrm{Cosh}\lambda_2 L - 1) & \left(1 + \frac{B}{\lambda_2(k^4 - BL)}\mathrm{Sinh}\lambda_2 L\right) \\ \sin\lambda_1 L & \cos\lambda_1 L - 1 & \mathrm{Sinh}\lambda_2 L & \mathrm{Cosh}\lambda_2 L - 1 \\ 0 & -\lambda_1^2 & 0 & \lambda_2^2 \\ -\lambda_1^2 \sin\lambda_1 L & -\lambda_1^2 \cos\lambda_1 L & \lambda_2^2 \mathrm{Sinh}\lambda_2 L & \lambda_2^2 \mathrm{Cosh}\lambda_2 L \end{vmatrix} = 0 \quad (5a)$$

Finally the shape functions are given by (4e) with:

$$\left.\begin{aligned} c_2 &= -c_1 \cdot \frac{\sin\lambda_1 L}{\cos\lambda_1 L - 1} \\ c_3 &= c_1 \cdot \left(\frac{\lambda_1}{\lambda_2}\right)^2 \cdot \frac{\sin\lambda_1 L \cdot (\mathrm{Cosh}\lambda_2 L - 1)}{\mathrm{Sinh}\lambda_2 L \cdot (\cos\lambda_1 L - 1)} \\ c_4 &= -c_1 \cdot \left(\frac{\lambda_1}{\lambda_2}\right)^2 \cdot \frac{\sin\lambda_1 L}{\cos\lambda_1 L - 1} \end{aligned}\right\} \quad (5b)$$

2.2 The deck

The deck of figure 4 has the following equation of motion:

$$EI_d w_d'''' + m\ddot{w}_d = p_z \quad (6a)$$

The shape functions are:

$$Z_n = \sin\frac{n\pi x}{L} \quad (6b)$$

and its eigenfrequencies are given by the formula:

$$\omega_{dn} = \sqrt{\frac{n^4 \pi^4 E I_d}{m_d L^4}} \tag{6c}$$

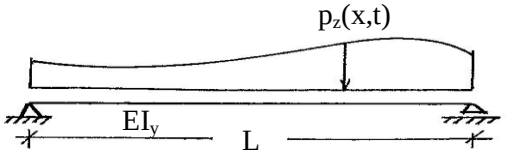

Figure 4. The deck

2.3 The cables

We consider a suspended arch bridge with two lines of cables.

It is valid that: $\sigma = \frac{q_z}{2A_c} = \varepsilon E_c = \frac{\Delta \ell}{\ell} \cdot E_c = \frac{w_d - w_a}{\ell} \cdot E_c$ which concludes to the following expression:

$$q_z(x,t) = \frac{2 E_c A_c}{z(x)} \cdot (w_d - w_a) \tag{7}$$

Where A_c is the area of the one line of the cables' cross-section per unit length of the deck and E_c is the modulus of elasticity of the cables.

3 THE 2D MODEL

3.1 Dense arrangement of cables

Let us consider now the suspended arch bridge shown in figure 5.
The following equations are valid:
For the arch

$$E I_c w_a'''' - \frac{m_a g L^2}{8 f_o} \cdot w_a'' + c \dot{w}_a + m_a \ddot{w}_a = q_z(x,t) - \frac{64 f_o}{K L^4} \cdot \int_0^L w_a dx \tag{8a}$$

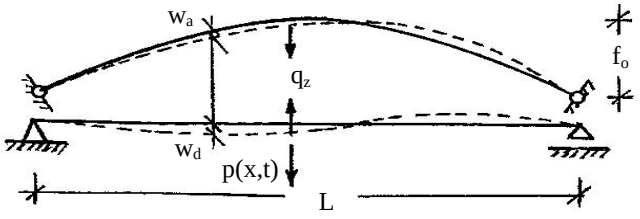

Figure 5. The suspended arch bridge

And for the deck

$$EI_d w_d'''' + c \cdot \dot{w}_d + m\ddot{w}_d = p_z(x,t) - q_z(x,t) \tag{8b}$$

Introducing $q_z(x,t)$ from equation (7) into equations (8a,b) we get:

$$\left.\begin{aligned} &EI_c w_a'''' - \frac{m_a g L^2}{8 f_o} \cdot w_a'' + \frac{2E_c A_c}{z(x)} w_a + c\dot{w}_a + m_a \ddot{w}_a = \frac{2E_c A_c}{z(x)} w_d - \frac{64 f_o}{K L^4} \cdot \int_0^L w_a dx \\ &EI_d w_d'''' + \frac{2E_c A_c}{z(x)} w_d + c \cdot \dot{w}_d + m_d \ddot{w}_d = p_z(x,t) + \frac{2E_c A_c}{z(x)} w_a \end{aligned}\right\} \tag{9a,b}$$

We are searching for a solution of the form:

$$\left.\begin{aligned} w_a(x,t) &= \sum_n W_n(x) \cdot T_n(t) \\ w_d(x,t) &= \sum_n Z_n(x) \cdot R_n(t) \end{aligned}\right\} \tag{10a,b}$$

where W_n from equation (4e) and Z_n from equation (6b), are the shape functions of the arch and the deck respectively, while T_n and R_n are time functions under determination.

Introducing the above expressions into equations (9a,b) we obtain:

$$\left.\begin{aligned} &EI_c \sum_n W_n'''' T_n - \frac{m_a g L^2}{8 f_o} \sum_n W_n'' T_n + \frac{2E_c A_c}{z(x)} \sum_n W_n T_n + c \sum_n W_n \dot{T}_n + m_a \sum_n W_n \ddot{T}_n = \\ &\qquad = \frac{2E_c A_c}{z(x)} \sum_n Z_n R_n - \frac{64 f_o^2}{K L^4} \int_0^L \sum_n W_n T_n dx \\ &EI_d \sum_n Z_n'''' R_n + \frac{2E_c A_c}{z(x)} \sum_n Z_n R_n + c \sum_n Z_n \dot{R}_n + m_d \sum_n Z_n \ddot{R}_n = p_z(x,t) + \frac{2E_c A_c}{z(x)} \sum_n W_n T_n \end{aligned}\right\} \tag{11a,b}$$

We remember that W_n and Z_n satisfy the following equations of the free motion:

$$\left.\begin{aligned} &EI_c W_n'''' - \frac{mgL^2}{8 f_o} W_n'' + m_a \omega_{an}^2 W_n = -\frac{64 f_o^2}{K L^4} \int_0^L W_n dx \\ &EI_d Z_n'''' - m_d \omega_{dn}^2 Z_n = 0 \end{aligned}\right\}$$

Therefore equations (11a,b) become:

$$\left.\begin{aligned} &m_a\sum_n W_n\ddot{T}_n + c\sum_n W_n\dot{T}_n + m_a\sum_n \omega_{an}^2 W_n T_n + \frac{2E_cA_c}{z(x)}\sum_n W_n T_n - \frac{2E_cA_c}{z(x)}\sum_n Z_n R_n = 0 \\ &m_d\sum_n Z_n\ddot{R}_n + c\cdot\sum_n Z_n\dot{R}_n + m_d\sum_n \omega_{dn}^2 Z_n R_n + \frac{2E_cA_c}{z(x)}\sum_n Z_n R_n - \frac{2E_cA_c}{z(x)}\sum_n W_n T_n = p_z(x,t) \end{aligned}\right\} \quad (12a,b)$$

Multiplying the first of (12) by W_ρ and integrating, the second of (12) by Z_ρ and integrating and taking into account the orthogonality conditions, we finally find:

$$\left.\begin{aligned} &\ddot{T}_\rho + \frac{c}{m_a}\dot{T}_\rho + \omega_{a\rho}^2 T_\rho + \Gamma_\rho\sum_n\left(T_n\int_0^L \frac{W_nW_\rho}{z(x)}dx\right) - \Gamma_\rho\sum_n\left(R_n\int_0^L\frac{Z_nW_\rho}{z(x)}dx\right) = 0 \\ &\ddot{R}_\rho + \frac{c}{m_d}\dot{R}_\rho + \omega_{d\rho}^2 R_\rho + \Delta_\rho\sum_n\left(R_n\int_0^L\frac{Z_nZ_\rho}{z(x)}dx\right) - \Delta_\rho\sum_n\left(T_n\int_0^L\frac{W_nZ_\rho}{z(x)}dx\right) = \frac{1}{m_d\int_0^L Z_\rho^2 dx}\int_0^L p_z Z_\rho dx \end{aligned}\right\} \quad (13a,b)$$

Without restriction of the generality, one can suppose that the following is valid:

$$p_z(x,t) = p_z(x)\cdot f_z(t) \quad (14)$$

In order to solve the system (13) we use the Laplace transformation, with initial conditions $R_\rho(0) = \dot{R}_\rho(0) = T_\rho(0) = \dot{T}_\rho(0) = 0$. We put:

$$\left.\begin{aligned} &LT_\rho(t) = \overline{T}_\rho(s), \qquad LR_\rho(t) = L\overline{R}_\rho(s) \\ &L\dot{T}_\rho(t) = s\cdot\overline{T}_\rho(s), \quad L\dot{R}_\rho(t) = s\cdot\overline{R}_\rho(s) \\ &L\ddot{T}_\rho(t) = s^2\cdot\overline{T}_\rho(s), \quad L\ddot{R}_\rho(t) = s^2\cdot\overline{R}_\rho(s) \\ &Lf_z(t) = \bar{f}_z(s) \end{aligned}\right\} \quad (15)$$

And also:

$$\left.\begin{aligned} &\alpha_{n\rho} = \Gamma_\rho\int_0^L\frac{W_nW_\rho}{z(x)}dx, \quad \beta_{n\rho} = \Gamma_\rho\int_0^L\frac{Z_nW_\rho}{z(x)}dx \\ &\gamma_{n\rho} = \Delta_\rho\int_0^L\frac{Z_nZ_\rho}{z(x)}dx, \quad \delta_{n\rho} = \Delta_\rho\int_0^L\frac{W_nZ_\rho}{z(x)}dx \\ &\varepsilon_\rho = \frac{\Delta_\rho}{2E_cA_c}\int_0^L p_z(x)\cdot Z_\rho dx \end{aligned}\right\} \quad (16)$$

Introducing the above equations (15) and (16) into (13) we obtain the following

linear system:

$$\left.\begin{aligned}
&\alpha_{1\rho}\overline{T}_1+....+(\alpha_{\rho\rho}+s^2+\frac{c}{m_a}s+\omega_{\alpha\rho}^2)\overline{T}_\rho+....+\alpha_{n\rho}\overline{T}_n-\beta_{1\rho}\overline{R}_1-....-\beta_{n\rho}\overline{R}_n=0\\
&\gamma_{1\rho}\overline{R}_1+....+(\gamma_{\rho\rho}+s^2+\frac{c}{m_d}s+\omega_{d\rho}^2)\overline{R}_\rho+....+\gamma_{n\rho}\overline{R}_n-\delta_{1\rho}\overline{T}_1-....-\delta_{n\rho}\overline{T}_n=\varepsilon\cdot\bar{f}_z
\end{aligned}\right\} \quad (17a,b)$$

with ρ=1 to n.
Solving the above system we determine $\overline{T}_\rho$ and $\overline{R}_\rho$ and further:

$$\left.\begin{aligned}
T_\rho(t)&=L^{-1}\overline{T}_\rho(s)\\
R_\rho(t)&=L^{-1}\overline{R}_\rho(s)
\end{aligned}\right\} \quad (18a,b)$$

3.2 Sparse arrangement of cables

One can Easily extend the above method in the case of a sparse arrangement of cables as follows:
The equation (7) that gives the cables' tensions is modified as follows:

$$q_z(x,t)=2E_cA_c\cdot\sum_{i=1}^{\sigma}\frac{w_d(x)-w_a(x)}{z(x)}\cdot\delta(x-\alpha_i) \quad (19)$$

where $\delta(x-\alpha)$ is the Dirac Delta function, α_i the position of the i^{th} cable and σ the number of cables. Therefore equations (9a,b) become:

$$\left.\begin{aligned}
&EI_cw_a''''-\frac{m_agL^2}{8f_o}\cdot w_a''+2E_cA_c\cdot\sum_{i=1}^{\sigma}\frac{w_a(x)}{z(x)}\cdot\delta(x-\alpha_i)+c\dot{w}_a+m_a\ddot{w}_a\\
&\qquad=2E_cA_c\cdot\sum_{i=1}^{\sigma}\frac{w_d(x)}{z(x)}\cdot\delta(x-\alpha_i)-\frac{64f_o}{KL^4}\cdot\int_0^L w_a\,dx\\
&EI_dw_d''''+2E_cA_c\cdot\sum_{i=1}^{\sigma}\frac{w_d(x)}{z(x)}\cdot\delta(x-\alpha_i)+c\cdot\dot{w}_d+m_d\ddot{w}_d=p_z(x,t)\\
&\qquad+2E_cA_c\cdot\sum_{i=1}^{\sigma}\frac{w_a(x)}{z(x)}\cdot\delta(x-\alpha_i)
\end{aligned}\right\} \quad 20(a,b)$$

We are searching for a solution like the one of equations (10a,b).
Introducing the expressions of (10a,b) into equations (9'a,b), taking into account the equations of free motion and following the procedure of §3.1 we conclude to the system (17a,b) where:

$$\left.\begin{aligned}
&\alpha_{n\rho}=\Gamma_\rho\cdot\sum_{i=1}^{\sigma}\frac{W_n(\alpha_i)W_\rho(\alpha_i)}{z(\alpha_i)},\quad \beta_{n\rho}=\Gamma_\rho\cdot\sum_{i=1}^{\sigma}\frac{Z_n(\alpha_i)W_\rho(\alpha_i)}{z(\alpha_i)}\\
&\gamma_{n\rho}=\Delta_\rho\cdot\sum_{i=1}^{\sigma}\frac{Z_n(\alpha_i)Z_\rho(\alpha_i)}{z(\alpha_i)},\quad \delta_{n\rho}=\Delta_\rho\cdot\sum_{i=1}^{\sigma}\frac{W_n(\alpha_i)Z_\rho(\alpha_i)}{z(\alpha_i)}\\
&\varepsilon_\rho=\frac{\Delta_\rho}{2E_cA_c}\int_0^L p_z(x)\cdot Z_\rho dx,\quad \Gamma_\rho=\frac{2E_cA_c}{m_a\int_0^L W_\rho^2 dx},\qquad \Delta_\rho=\frac{2E_cA_c}{m_d\int_0^L Z_\rho^2 dx}
\end{aligned}\right\}\qquad (21)$$

Therefore solving the system (17a,b) we determine $\overline{T}_\rho$ and $\overline{R}_\rho$ and further from (18a,b) the time functions T_ρ and R_ρ.

4 NUMERICAL EXAMPLES AND DISCUSSION

Let us consider us a suspended arch bridge like the one of figure 5.

The bridge is made for isotropic homogeneous material with modulus of elasticity $E_s=2.1\cdot10^8\,kN/m^2$ and shear modulus $G=0.8\cdot10^8\,kN/m^2$.

The length of the bridge is $L=120m$ and its width $2b=10m$.

For the arch we have $f_o=18m$, $I_c=0.2m^4$ and $m_a=300kg/m$.

For the deck we have moments of inertia in bending $I_y=0.03m^4$ and mass per unit length $m_d=200kg/m$.

The cables are placed in two rows at the edge of the cross-section of the bridge having area per unit step $A_c=3.0\cdot10^{-4}\,m^2/m/row$, and modulus of elasticity $E_c=1.5\cdot10^8\,kN/m^2$.

An initial elevation has been given to the deck by prestressing of the cables according to the following expression: $\upsilon_{do}=0.001\cdot\sin\frac{\pi x}{L}$.

At t=0, a moving concentrated load F=600 kN or a distributed one p=20 kN/m^2 enters the bridge moving with velocity v, and acting centrically or eccentrically.

4.1 The moving concentrated load

Considering firstly a concentrated load of F=600 kN moving on the axis of the deck with constant velocity v=20 m/sec (or else 72 km/h) and applying the formulae of §3 we obtain the following plots of figures 7 and 8.

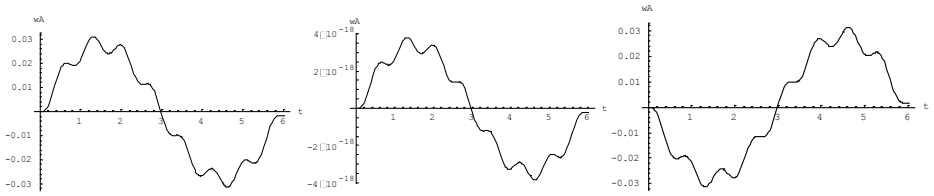

Figure 7. The motion of the arch's first quarter, middle, and third quarter

From the above plots, we verify that always the arch is deformed in anti symmetrical forms which the middle point has negligible motion.

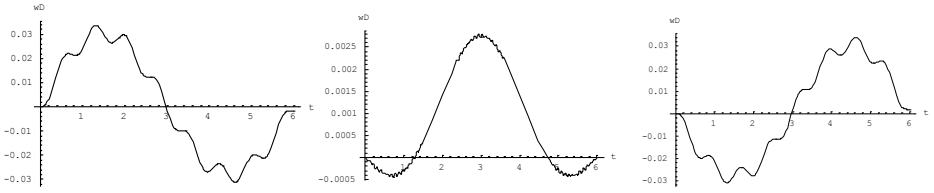

Figure 8. The motion of the deck's first quarter, middle, and third quarter

The motion of the deck's first quarter, middle and third quarter are shown in figure 8, while the tensions of the cables are shown in figure 9 for different time instants.

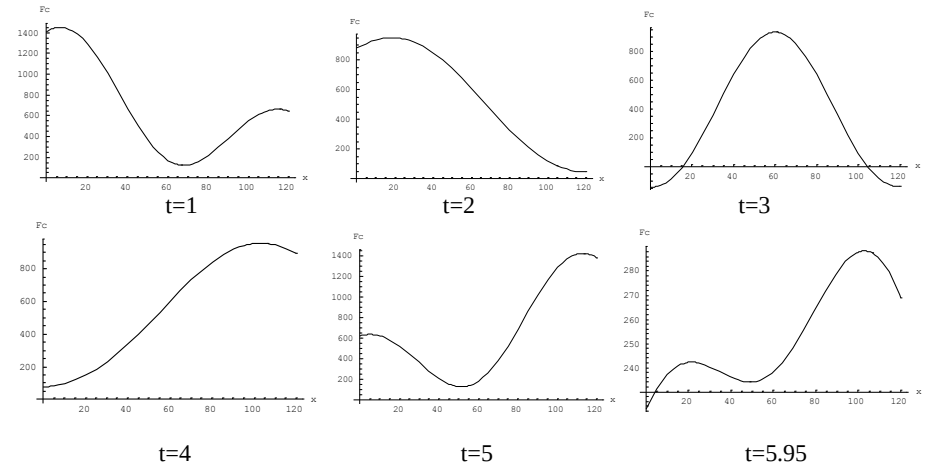

Figure 9. The cables forces at different time instants

4.2 The moving distributed load

Considering now a distributed load of p=20 kN/m^2, acting on a width of 2 meters, moving on the axis of the deck with constant velocity v=20 m/sec (or else 72 km/h) and applying the formulae of §3 we obtain the following plots of figures 10, 11 and 12.

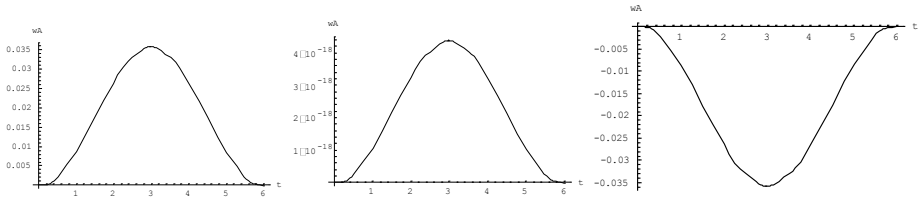

x=L/4 x=L/2 x=3L/4

Figure 10. The motion of the arch's first quarter, middle and third quarter

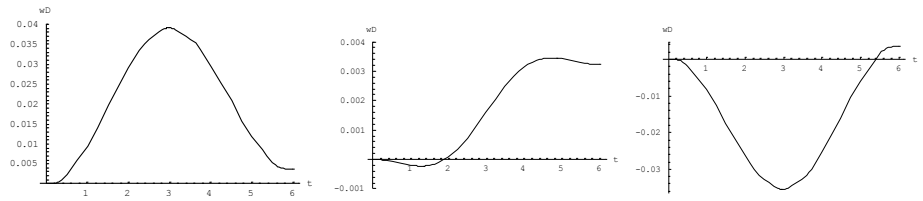

x=L/4 x=L/2 x=3L/4

Figure 11. The motion of the deck's first quarter, middle and third quarter

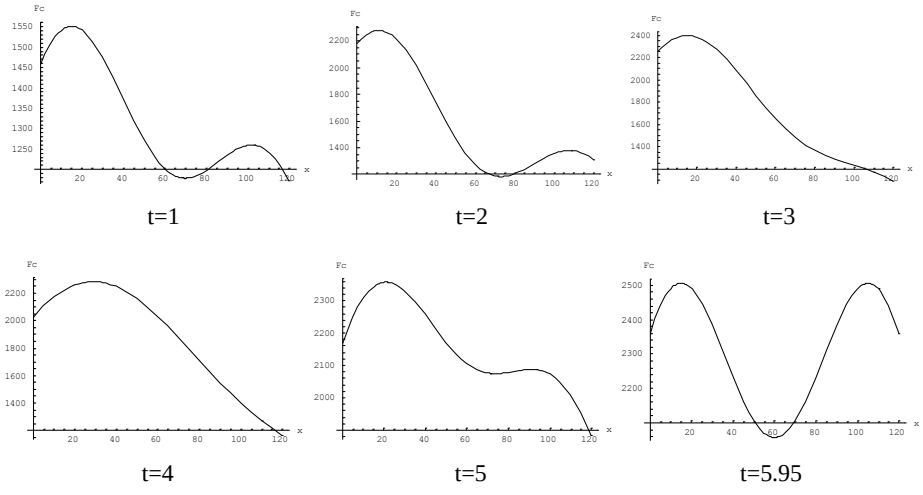

t=1 t=2 t=3

t=4 t=5 t=5.95

Figure 12. The cables forces at different time instants

5 CONCLUSIONS

From the results of the model considered, one can draw the following conclusions.

1. A mathematical model is proposed either for the 2D distress and for the 3D distress of the bridge. The above model with densely placed cables can also be easily applied for sparse cables installation.
2. The specific behavior of the arch, which is always deformed into anti symmetrical shapes, has been verified, while its midpoint at x=L/2 remains practically immovable having negligible motion, as one can be seen in figures 7 and 10.
3. Although the total distributed load is less than the concentrated one, it causes greater tensions on the cables, perhaps because it acts, each time, on a larger part of the deck.
4. Both concentrated or distributed moving loads cause the largest stressing of the cables and the greatest difference between the stressing of the two rows of cables when entering or exiting the bridge.

REFERENCES

[1] Johnston B.G. "Guide to stability design criteria for metal structures", Structural Stability Research Council, 3rd edition, John Wiley & Sons, N.Y., 1976

[2] Bergmeister, K., Capsoni, A., Corradi, L., Menardo, A. "Lateral elastic stability of slender arches for bridges including deck slenderness", Structural Engineering International: Journal of the International Association for Bridge and Structural Engineering (IABSE), 19 (2), pp. 149-154, 2009

[3] Pircher, M., Stacha, M., Wagner, J. "Stability of network arch bridges under traffic loading" Proceedings of the Institution of Civil Engineers: Bridge Engineering 166 (3), pp. 186-192, 2013

[4] Wang, Y., Liu, C., Liang, Y., Zhang, S. "Nonlinear stability analysis and completed bridge test on slanting type CFST arch bridges", Source of the Document Jianzhu Jiegou Xuebao/Journal of Building Structures 36, pp. 107-113, 2015

[5] Zhu, X.-L., Sun, D.-B. "Nonlinear in-plane stability and catastrophe analysis of shallow arches", Zhendong yu Chongji/Journal of Vibration and Shock 35 (6), pp. 47-51 and 74, 2016[6] Bruno, D., Lonetti, P., Pascuzzo, A. "Document An optimization model for the design of network arch bridges", Computers and Structures 170, pp. 13-25, 2016

[6] Mannini, C., Belloli, M., Marra, A.M., (...), Robustelli, F., Bartoli, G. "Aeroelastic stability of two long-span arch structures: A collaborative experience in two wind tunnel facilities", Engineering Structures 119, pp. 252-263, 2016

[7] Zhang, Z.-C. "Creep analysis of long span concrete-filled steel tubular arch bridges", Gongcheng Lixue/Engineering Mechanics 24 (5), pp. 151-160, 2007

[8] Shao, X., Peng, J., Li, L., Yan, B., Hu, J. "Time-dependent behavior of concrete-filled steel tubular arch bridge", Journal of Bridge Engineering 15 (1), pp. 98-107, 2010

[9] Loghman, A., Ghorbanpour Arani, A., Shajari, A.R., Amir, S. "Time-dependent thermoelastic creep analysis of rotating disk made of Al-SiC composite", Archive of Applied Mechanics 81 (12), pp. 1853-1864, 2011

[10] Lai, X.-Y., Li, S.-Y., Chen, B.-C., "The influence of addictives on the creep of concrete-filled steel tube", Harbin Gongye Daxue Xuebao/Journal of Harbin Institute of Technology 44 (SUPPL.1), pp. 248-251, 2012

[11] Granata, M.F., Arici, M. "Serviceability of segmental concrete arch-frame bridges built by

cantilevering", Bridge Structures 9 (1), pp. 21-36, 2013
[12] Ma, Y.S., Wang, Y.F. "Creep effects on the reliability of a concrete-filled steel tube arch bridge", Journal of Bridge Engineering 18 (10), pp. 1095-1104, 2013
[13] Zhou, Y. "Concrete creep and thermal effects on the dynamic behavior of a concrete-filled steel tube arch bridge", Journal of Vibroengineering 16 (4), pp. 1735-1744, 2014
[14] Bradford, M.A., Pi, Y.-L. "Geometric Nonlinearity and Long-Term Behavior of Crown-Pinned CFST Arches", Journal of Structural Engineering (United States) 141 (8), 04014190, 2015
[15] Li, J.-B., Ge, S.-J., Chen, H. "Document Seismic behavior analysis of a 5-span continuous half-through CFST arch bridge", World Information on Earthquake Engineering 21(3) pp110-115, 2005
[16] Álvarez, J.J., Aparicio, A.C., Jara, J.M., Jara, M. "Seismic assessment of a long-span arch bridge considering the variation in axial forces induced by earthquakes", Engineering Structures 34, pp. 69-80, 2012
[17] Huang, F.-Y., Chen, B.-C., Li, J.-Z., Cheng, H.-D. "Shaking tables testing of concrete filled steel tubular single arch rib model under the excitation of rare earthquakes", Gongcheng Lixue/Engineering Mechanics 32 (7), pp. 64-73, 2015
[18] Sevim, B., Atamturktur, S., Altunişik, A.C., Bayraktar, A. "Ambient vibration testing and seismic behavior of historical arch bridges under near and far fault ground motions", Bulletin of Earthquake Engineering , 14(1), 241-259, 2016
[19] Lei, S., Gao, Y., Pan, D. "An optimization solution of Rayleigh damping coefficients on arch bridges with closely-spaced natural frequencies subjected to seismic excitations", Harbin Gongye Daxue Xuebao/Journal of Harbin Institute of Technology 47 (12), pp. 123-128, 2015
[20] Drosopoulos, G.A., Stavroulakis, G.E., Massalas, C.V. "Influence of the geometry and the abutments movement on the collapse of stone arch bridges", Construction and Building Materials 22 (3), pp. 200-210, 2008
[21] Liu, B., Yang, C., Zhou, K. "Document Effect of springing displacement on mechanical performance of the buried corrugated steel arch bridge", Wuhan Ligong Daxue Xuebao (Jiaotong Kexue Yu Gongcheng Ban)/Journal of Wuhan University of Technology (Transportation Science and Engineering) 36 (3), pp. 441-444, 2012
[22] Liu, S.-M., Wang, Z.-X., Zhu, C. "Method of temporarily carrying heavy vehicle on masonry arch bridge without strengthening", Beijing Gongye Daxue Xuebao/Journal of Beijing University of Technology 41 (10), pp. 1559-1565, 2015
[23] Yau, J.-D. "Vibration of parabolic tied-arch beams due to moving loads", Document International Journal of Structural Stability and Dynamics, 6 (2), pp. 193-214, 2006
[24] Yang, J.-X., Chen, W.-Z., Gu, R. "Analysis of dynamic characteristics of short hangers of arch bridge", Bridge Construction 44 (3), pp. 13-18, 2014
[25] Nikkhoo, A., Kananipour, H., "Document Numerical solution for dynamic analysis of semicircular curved beams acted upon by moving loads", Proceedings of the Institution of Mechanical Engineers, Part C: Journal of Mechanical Engineering Science 228 (13), pp. 2314-2322. 2014
[26] Türker, T., Bayraktar, A. "Structural safety assessment of bowstring type RC arch bridges using ambient vibration testing and finite element model calibration", Measurement: Journal of the International Measurement Confederation pp 33-45, 2014
[27] Calçada, R., Cunha, A., Delgado, R., "Dynamic analysis of metallic arch railway bridge", Journal of Bridge Engineering 7 (4), pp. 214-222, 2002
[28] Chen, S., Tang, Y., Huang, W.-J., "Visual vibration simulation of framed arch bridge under multi-vehicle condition", Gongcheng Lixue/Engineering Mechanics 22 (1), pp. 218-222, 2005
[29] Wallin, J., Leander, J., Karoumi, R. "Strengthening of a steel railway bridge and its impact on the dynamic response to passing trains", Engineering Structures 33 (2), pp. 635-646, 2011